DIGITAL EMULATION OF DISTORTION EFFECTS BY WAVE AND PHASE SHAPING METHODS

Joseph Timoney[†], *Victor Lazzarini*[†], *Anthony Gibney*[†]
and Jussi Pekonen [††]

[†]Sound and Music Technology Group
National University of Ireland

Maynooth, Ireland
jtimoney@cs.nuim.ie,
victor.lazzarini@nuim.ie

[††]Dept. Signal Processing and Acoustics
Aalto University School of Science and Technology
Espoo, Finland
jussi.pekonen@tkk.fi

ABSTRACT

This paper will consider wave and phase signal shaping techniques for the digital emulation of distortion effect processing. We examine in detail how to determine the wave and phase shaping functions with harmonic amplitude data only first, and then after including the harmonic phase data. Three distortion effects units are used to provide test data. Wave and phase shaping functions for the emulation of these effects are derived with the assistance of a super-resolution frequency-domain analysis technique. In complement to this, we describe an alternative time domain method for determining phase shaping functions using Dynamic Time Warping. Finally, we propose a method for assessing the frequency dependency of distortion effects to help the design of multiband wave and phase shaping functions.

1. INTRODUCTION

Since the mid 1960s, distortion effects have played an important part in the timbristic definition of electric guitar sounds in popular music. Such effects have also been applied to organ and synthesizer sounds. For instance, when used with the Hammond organ, it creates thick, harmonic-rich tone. Another notable use is with the Roland TB303 bass synthesizer, producing what can be described as a screaming sound when the filter is fully open and the resonance control is at a maximum. The origin of such effects can be traced back to musicians exceeding the linear dynamic range of tube amplifiers, introducing some sort of non-linear distortion in the signal path. The characteristics of tube distortion provided a desirable transformation to the sound of instruments by adding high-frequency harmonics [1], [2]. In time, various types of dedicated circuitry were designed to apply different forms of the effect to signals at any amplitude level.

Distortion units essentially are a non-linear waveshaping circuit to alter the shape of the input thereby modifying its spectrum, typically using some form of diode-based clipping [3], [4]. Digital emulation of these analogue processes has appeared in a variety of forms. In some, the aim is to directly model a specific analogue circuit to reproduce its behavior [5], while in others the aim is to create algorithms that capture the analogue processing in a conceptual manner [6], [7], [8]. The advantages of the latter approach are flexibility, in terms of the potential for added features, and the ability to control the use of use of oversampling, which is a necessity for circuit modeling [9]. Furthermore, by keeping an algorithm's computational requirements low means many more instances of it can be used in parallel within a digital music production environment. Emulation using the algorithmic approach can be divided into a nonlinear system model with memory or without memory [9]. However, incorporating memory for systems with strong nonlinearities is computationally expensive for real-time synthesis [10]. Thus, it is more common to use a nonlinear system that is memoryless.

The action of such a nonlinear system is understood as waveshaping [11], a form of amplitude distortion. It has been shown more recently that distortion can also be applied to the signal phase to achieve a similar result [12], [13], [14], although no complete theory for this is available. In this work we establish a connection between the wave and phase shaping methods of amplitude and phase distortion [15] respectively. To illustrate the analysis, examples of nonlinearly shaped sinusoids that have been processed using analogue distortion effects will be used. Additionally, in reference to the multiband extension of waveshaping [16], an idea for examining the variation in shaping with respect to input sinusoid frequency will be introduced.

This paper is organised as follows. We will first introduce and discuss the amplitude and phase signal shaping techniques. Then we will examine three distortion effects, discussing the general principles behind their operation. This will be followed by the application of the previously discussed algorithms to emulate these effects, with parameters derived from the analyses of their output signals. A brief description will also be made of using DTW as pure time domain approach to implement phase shaping. To finish the paper, we will look at ways to examine and describe the frequency dependency of these effects for potential applications in multiband processing.

2. SIGNAL SHAPING METHODS

2.1. Non-linear waveshaping

One of the first studies of digital waveshaping in the literature is found in Schaefer's work on tone generation [11]. However, J. C. Risset had already been using the method for sound synthesis of complex time-varying waveforms with a digital computer [17]. Schaefer's motivation was the modeling of nonlinear semiconductor elements used in electronic musical devices. Thorough theoretical investigations followed in [18] and [19]. The basic idea is that given some sinewave at a frequency ω

$$x(t) = \cos(\omega t) \tag{1}$$

there is a nonlinear function *f*(.) that will alter the amplitude of *x*(*t*) to produce an output

$$y(t) = f\big(x(t)\big) = f\big(\cos(\omega t)\big) \tag{2}$$

Thus, the shape of the input wave has been changed by the function.

In [11] Chebyshev polynomials were introduced as a useful description for such nonlinearities. The output of eq. 2 can be written as a power series

$$y(t) = d_0 + d_1\cos(\omega t) + d_2\cos^2(\omega t) + \ldots \tag{3}$$

or more compactly

$$y(t) = \sum_{p=0}^{\infty} d_p x^p(t) \tag{4}$$

Using a Fourier decomposition to determine the coefficients of eq.4 is difficult because of the expansion of the trigonometric product terms. The useful property of Chebyshev polynomials is that

$$T_k\big(\cos(\omega t)\big) = \cos(k\omega t) \tag{5}$$

where T_k denotes a Chebyshev polynomial of order *k*. Applying these polynomials to describe eq. 4 results in

$$y(t) = \frac{a_0}{2}T_0 + a_1T_1 + a_2T_2 + \ldots + a_NT_N \tag{6}$$

where a_0, a_1, a_2 ... are the Fourier series coefficient of *y(t)*.

The original work of [11] was extended by [19] to the synthesis of complex dynamic spectra. In particular, [19] provided a matrix based technique for computing the coefficients of the power series in eq.4 using the Fourier series coefficients of eq.6. This simplified the procedure for calculating the waveshaping transfer function given a set of spectral harmonic magnitudes. Using an (*N*+1)×(*N*+1) generative matrix *P* the relationship is

$$\begin{bmatrix} d_0 \\ d_1 \\ \vdots \\ d_N \end{bmatrix} = 0.5 \begin{bmatrix} (2)^0 \\ (2)^1 \\ \vdots \\ (2)^N \end{bmatrix} P \begin{bmatrix} a_0 \\ a_1 \\ \vdots \\ a_N \end{bmatrix} \tag{7}$$

The first row of the generative matrix *P* is

$$p(1,j) = \begin{bmatrix} 1 & 0 & -2 & 0 & 2 & 0 & -2 \ldots \end{bmatrix} \tag{8}$$

and subsequent rows can be computed using the recursion

$$p(i,j) = p(i-1,j-1) - p(i,j-2) \tag{9}$$

It can be noted from eq.7 that the harmonic phase is missing from the relationship. To include this means a phase quadrature form of waveshaping [18]. Each harmonic magnitude, except the DC component, has an associated phase. Defining these as

$$\boldsymbol{\varphi} = \begin{bmatrix} \phi_0 & \phi_1 & \phi_2 \ldots \phi_N \end{bmatrix} \tag{10}$$

To take account of the phase two waveshaping polynomials now need to be generated. Furthermore, the second polynomial requires Chebyshev polynomials of the second kind. Again, following the example of [19] matrix relationships can be expressed for phase quadrature waveshaping

$$\begin{bmatrix} dI_0 \\ dI_1 \\ \vdots \\ dI_N \end{bmatrix} = 0.5 \begin{bmatrix} (2)^0 \\ (2)^1 \\ \vdots \\ (2)^N \end{bmatrix} P \begin{bmatrix} a_0\cos(-\phi_0) \\ a_1\cos(-\phi_1) \\ \vdots \\ a_N\cos(-\phi_N) \end{bmatrix} \tag{11}$$

and

$$\begin{bmatrix} dQ_0 \\ \vdots \\ dQ_{N-1} \end{bmatrix} = 0.5 \begin{bmatrix} (2)^1 \\ \vdots \\ (2)^N \end{bmatrix} Q \begin{bmatrix} a_1\sin(-\phi_1) \\ \vdots \\ a_N\sin(-\phi_N) \end{bmatrix} \tag{12}$$

where the first row of the generative matrix *Q* is

$$q(1,j) = \begin{bmatrix} 1 & 0 & -1 & 0 & 1 & 0 & -1 \ldots \end{bmatrix} \tag{13}$$

and subsequent rows can be computed using the recursion

$$q(i,j) = q(i-1,j-1) - q(i,j-2) \tag{14}$$

The quadrature waveshaper output is then given by

$$y(t) = \sum_{p=0}^{\infty} dI_p x^p(t) + \sin(\omega t)\sum_{p=0}^{\infty} dQ_p x^p(t) \tag{15}$$

2.2. First relationship between wave and phase shaping

LeBrun [18] also provided a waveshaping implementation of Frequency Modulation (FM) synthesis [20] (normally described in the form of Phase Modulation, PM). This was a significant result as it first established the link between waveshaping, an amplitude based shaping technique, with frequency modulation, a phase-based shaping technique.

In outline, a FM (PM) signal can be written as

$$s(t) = \cos\big(\omega_c t + I\cos(\omega_m t)\big) \tag{16}$$

where ω_c is the carrier frequency, ω_m is the carrier frequency and *I* is the index of modulation.

Ignoring the carrier for the moment, eq.16 can be written as

$$\alpha(t) = \cos\big(I\cos(\omega_m t)\big) \tag{17}$$

Substituting eq.1 into eq.17 gives

$$\alpha(t) = \cos\big(Ix_m(t)\big) \tag{18}$$

This is similar to eq.(2) with the waveshaping function

$$f(x) = \cos(x) \tag{19}$$

The carrier can also be reintroduced to give

$$s(t) = \cos(\omega_c t) f\left(Ix_m(t)\right) - \sin(\omega_c t) g\left(Ix_m(t)\right) \tag{20}$$

with $g(x) = \sin(x)$.

Thus demonstrating frequency modulation can be cast as a form of waveshaping. The work in [21] elaborates this further, expanding it to provide independent control over partial groups. However, for our purpose more analysis is needed to have an equivalent procedure for computing the phase shaping function given a set of harmonic amplitudes and phases.

2.3. Non-linear phaseshaping

The technique of phase distortion, which is the core of our phase-shaping approach, was originally proposed as a digital synthesis method for the generation of complex time-varying tones [15]. More recently, in [13] and [14], it was explored as an efficient alternative for the design of virtual analogue oscillators. In [12] it was proposed to implement it using allpass filters as an effect for distorting sinewaves, though in principle it could be applied to any allpass filter input.

As discussed in Section 2.2, the similarities between wave and phase shaping are substantial. To establish the connection fully, we again start with the same sinusoidal signal of eq. 4, and propose that there is a non-linear function $f(.)$ such that

$$y(t) = \cos\left(f(\omega t)\right) \tag{21}$$

will produce a complex signal. A detailed analysis of its spectrum is found in [14]. In a typical scenario, $f(.)$ will be such that the result signal will be equivalent to a complex-FM tone. More importantly for this work, it is also possible to establish a connection between the harmonic magnitudes of a signal and its instantaneous phase. First, defining a N harmonic analytic signal of fundamental frequency ω and amplitudes $a_1 ... a_N$ as

$$s(t) = a_1 e^{\omega t} + a_2 e^{2\omega t} + a_3 e^{3\omega t} + \ldots + a_N e^{N\omega t} \tag{22}$$

This can be written as into its real and imaginary components

$$s(t) = u(t) + jv(t) \tag{23}$$

where $u(t)$ and $v(t)$ denote the real and imaginary parts respectively. If the relationship between the harmonic magnitudes satisfies the conditions given in [22], then the instantaneous frequency of this signal can be written as [23]

$$\dot{\phi}_s(t) = \frac{u(t)\dot{v}(t) - \dot{u}(t)v(t)}{A^2} \tag{24}$$

where $\dot{u}(t)$ and $\dot{v}(t)$ are the first differences of the real and imaginary parts, respectively, and

$$A = \sqrt{u^2(t) + v^2(t)} \tag{25}$$

Substituting for $u(t)$, $v(t)$, $\dot{u}(t)$ and $\dot{v}(t)$ the above will lead to an expression from which the Instantaneous frequency can be directly calculated.

Defining the combination

$$\mathbf{C} = \binom{N}{2} \tag{26}$$

This will have the set of combinadics denote $\mathbf{M}_{(N,2)}$ that contains $L = N!/(2!(N-2)!)$ vectors each denoted as $M_{(N,2)}(.)$. Also, the vectors of magnitudes and frequencies are

$$\mathbf{a} = \left[a_1 a_2 \ldots a_N\right] \tag{27a}$$

and

$$\boldsymbol{\omega} = \left[\omega\ 2\omega \ldots N\omega\right] \tag{27b}$$

Then, defining two terms

$$\phi_{s\,num}(t) = \sum_{i=1}^{L} \mathbf{a}^2 . \boldsymbol{\omega} + \sum_{i=1}^{L} \boldsymbol{\omega}\left(M_{N,2}(i)\right) \mathbf{a}\left(M_{N,2}(i)\right) \cos\left(\boldsymbol{\omega}'\left(M_{N,2}(i)\right) t\right) \tag{28a}$$

where $\boldsymbol{\omega}'$ is the difference between the pair of frequencies determined by $M_{(N,2)}(.)$ and

$$\phi_{s\,den}(t) = \sum_{i=1}^{L} \mathbf{a}^2 + \sum_{i=1}^{L} 2\,\mathbf{a}\left(M_{N,2}(i)\right) \cos\left(\boldsymbol{\omega}'\left(M_{N,2}(i)\right) t\right) \tag{28b}$$

The instantaneous frequency is given by

$$\dot{\phi}_s(t) = \frac{\dot{\phi}_{s\,num}(t)}{\dot{\phi}_{s\,den}(t)} \tag{29}$$

The instantaneous frequency can be written in terms of the fundamental frequency and frequency deviation

$$\dot{\phi}_s(t) = \omega + \dot{\phi}_{s\,dev}(t) \tag{30}$$

This deviation term can be integrated to convert it into an equivalent modulation or phase shaping

$$\phi_{s\,\mathrm{mod}}(t) = \sum_{n} \dot{\phi}_{s\,dev}(t) \tag{31}$$

Thus it is possible to represent a harmonic signal as the phase shaping of a cosine signal at the same fundamental frequency.

No harmonic phases have been taken into account so far and the equations need to be extended to achieve this. Using our phase vector definition in eq. 10, the terms in eq. 28a and 28b can be redefined

$$\phi_{snum}(t) = \sum_{i=1}^{L} \mathbf{a}^2 .\boldsymbol{\omega} + \sum_{i=1}^{L} \boldsymbol{\omega}\left(M_{N,2}(i)\right)\mathbf{a}\left(M_{N,2}(i)\right)\cos\left(\boldsymbol{\varphi}'\left(M_{N,2}(i)\right) + \boldsymbol{\omega}'\left(M_{N,2}(i)\right) t\right) \quad (32a)$$

where $\boldsymbol{\varphi}'$ is the difference between the pair of phases determined by $\boldsymbol{M}_{(N,2)}(.)$ and

$$\phi_{sden}(t) = \sum_{i=1}^{L} \mathbf{a}^2 + \sum_{i=1}^{L} 2\,\mathbf{a}\left(M_{N,2}(i)\right)\cos\left(\boldsymbol{\varphi}'\left(M_{N,2}(i)\right) + \boldsymbol{\omega}'\left(M_{N,2}(i)\right) t\right) \quad (32b)$$

These can be substituted into eq.29, eq. 30 and eq. 31 to find the phase shaping that will produce the signal *s(t)*.

3. THE DISTORTION EFFECTS

Distortion is a waveshaping operation, altering the contour of its input, and therefore its harmonic content. In transistor-based distortion effects the primary circuit element that alters the signal is the diode. Two broad classes of circuits exist: (a) Hard clipping and (b) Soft clipping [3], [4]. While hard clipping cuts the peaks of the input signal to create a strong distortion, soft clipping enacts this in a gentler manner producing a warmer, overdriven sound. For this work, three distortion circuits were used. These were built from schematics and PCBs purchased from [24]. The schematics are available on the website [24]. The first was *El Griton*, a Tubescreamer-type circuit that gave an asymmetrical soft clipping. The second was *Disto-Uno*, a Boss DS-1 type circuit and the third was *MAS Distortion*, a MXR distortion-type circuit, both of which were hard clippers. These circuits will be termed as 'Overdrive', 'Clipper 1' and 'Clipper 2' in the following. The output waveform from all three circuits is shown in fig 1. The circuits were driven by a 2V peak-peak sinewave at frequency 146.8 Hz (note D) and the output was sampled at 44100Hz using an M-audio Audiophile soundcard. The three panels from top to bottom show the waveforms for the Overdrive, Clipper 1 and Clipper 2 respectively.

In fig. 1 the soft clipping action of the Overdrive contrasts to the hard clipping of the others as some of the roundness of the input sinewave is still visible in the output. The waveform of Clipper 1 is very strongly clipped and also has two significant transients each period. The Clipper 2 output appears to be the result of a straightforward clipping operation. Fig. 2 plots the normalized magnitude spectra of these three waves from 0Hz to 5000 Hz. The spectrum of Clipper 1 in the middle panel has the most harmonics implying it has the most distorted sound. The strong high frequency harmonics are most likely the result of the transients. The spectrum of the Overdrive in the top panel has the least number of high frequency harmonics and the fundamental component is at least 20dB stronger than any of the others.

The spectrum of Clipper 2 output is not the same as that of a square wave but it may be more similar to that of a pulse-width modulation (PWM) wave as it appears to have spectral minima around approximately 1800 Hz, 2800 Hz, 3800 Hz and 4800 Hz.

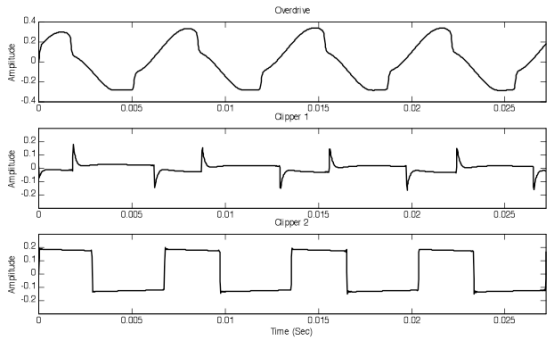

Figure 1: *Waveform outputs from the three distortion circuits fed by a sinewave signal.*

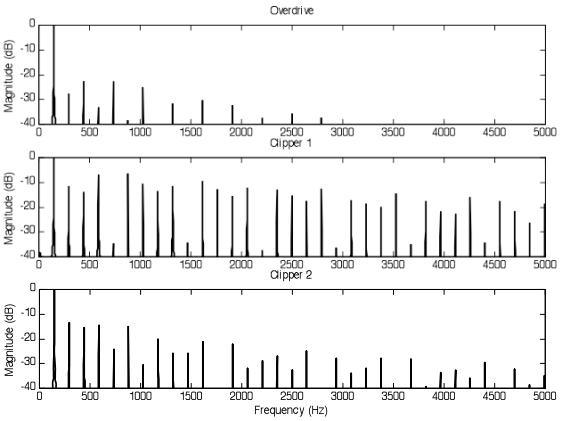

Figure 2: *Magnitude spectra of outputs from the three distortion circuits*

4. DIGITAL MODELLING BY MEANS OF WAVE AND PHASE SHAPING

Once the output waveforms were recorded the next task was to find the spectral peaks for input to the amplitude and phase shaping algorithms. However, to use the FFT for this would require a very long dataset as the fundamental frequency of the output was 146.8Hz. To overcome this, a super-resolution frequency analysis technique was applied. Exact values for the harmonic magnitudes and phases of the measured waveforms were derived using the Complex Spectral Phase Evolution (CSPE) algorithm [25]. Its algorithm can be described as follows:

Firstly, assume a real signal *s0*(*t*), and a one-sample shifted version of this signal *s1*(*t*). Also, its frequency is $\beta = q + \delta$ where *q* is an integer and δ is a fractional number. If *w*(*t*) a window function, *Fws0* is windowed Fourier transform of *s0*(*t*), and *Fws1* is the windowed Fourier transform of *s1*(*t*), then, from [25], first define

$$D = e^{\frac{j2\pi\beta}{N}} \quad (33)$$

The frequency dependent CSPE function can be written as

$$CSPE_w = F_{ws_0} F^*_{ws_1} = (\frac{a}{2})^2 \begin{bmatrix} D^* \left\| F_w(D^n) \right\|^2 \\ +2\mathrm{Re}\left\{ e^{j2b} D F_w(D^n) \otimes F_w{}^*(D^{-n}) \right\} \\ +D \left\| F_w(D^{-n}) \right\|^2 \end{bmatrix} \tag{34}$$

The windowed transform requires multiplication of the time domain data by the analysis widow, and thus the resulting transform is the convolution of the transform of the window function with the transform of a complex sinusoid. Since the transform of a complex sinusoid is a pair of delta functions in the positive and negative frequency positions, the result of the convolution is merely a frequency-translated copy of the window function frequency response centred at +β and -β. Consequently, with a standard windowing function, the $\|Fw\ (D^n)\|$ term is only considerable when $k \approx \beta$ and it decays rapidly when k is far from β. If the analysis window is chosen carefully so that it decays rapidly to minimize any spectral leakage into adjacent bins, the second and third terms become negligible in eq. 34. Thus, the CSPE for the positive frequencies gives:

$$CSPE_w \approx \frac{a^2}{4} \left\| F_w(D^n) \right\|^2 D^{-1} \tag{35}$$

From eq. 35 the CSPE exact frequency value is obtained

$$f_{CSPE} = \frac{-N\angle(CSPE_w)}{2\pi} = \frac{-N\angle(\frac{a^2}{4} \left\| F_w(D^n) \right\|^2 e^{-j\frac{2\pi}{N}\beta})}{2\pi} = \beta \tag{36}$$

In addition to providing an exact frequency measurement, with the CSPE, the amplitude and phase of the *k*th frequency component can be found using the following equations, where *W(ω-fcspe(k))* is the Fourier Transform of window function which has been shifted to *fcspe(k)* in frequency domain [25]:

$$A_k = \left\| \frac{2F_{ws_0}}{W(\omega - fcspe(k))} \right\| \tag{37}$$

$$\phi_k = \angle\left(\frac{2F_{ws_0}}{W(\omega - fcspe(k))} \right) \tag{38}$$

Empirically it was found that 40 harmonics only were required from the spectrum of the Overdrive for the analysis, otherwise the output of the waveshaper (eq. 4) was prone to instability. It was the weakness of the higher harmonics that gave rise to this. The magnitude of the 40th harmonic relative to the fundamental was -60dB so the timbral reproduction should not be overly compromised. To be consistent the same upper limit on the number of harmonics was used for the others also.

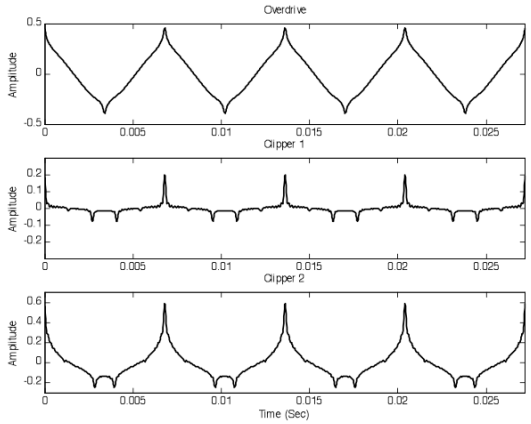

Figure 3: *Output of the standard waveshaper*

For the first emulation no harmonic phases were included. The output of the waveshaper formed using eq. 7 and 3 for all three waves is given in fig. 3. Clearly, by omitting the phase the original waveform shape is lost.

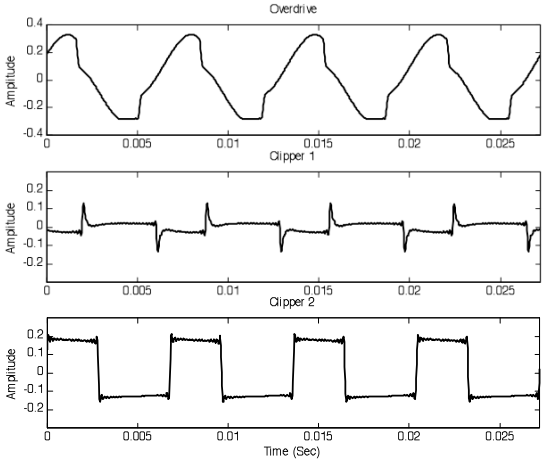

Figure 4: *Output of the phase quadrature waveshaper*

Using the phase quadrature waveshaping with eq. 11, 12 and 15, and thus including the phase, produces the plot in fig. 4. The reproduction of the original waveshape is much better now and they compare very well to the originals in fig. 1. Computing eqs. 28-31 with the harmonic magnitudes only the phase shaping function was computed for the three waveforms. Fig. 5 shows the output.

The phase shaping for the Overdrive is the smoothest function. This suggests that it might not be difficult to find a low order parametric model for this function. However, the phase shaping functions for the others are more jagged, implying that modelling might be more difficult.

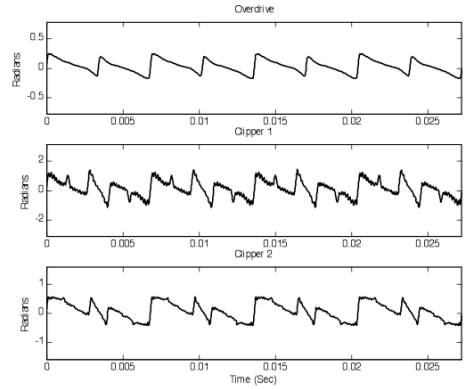

Figure 5: *Phase shaping function computed using harmonic magnitudes only*

Fig. 6 plots the phase shaping functions when the phase information is included using eqs. 32a and 32b. All three functions appear smoother. Notably the phase excursion for the Clipper 1 is greatest whilst that for the Overdrive is smallest. The phase shaping function for Clipper 2 is like a succession of sawtooths whose periods alternate between long and short.

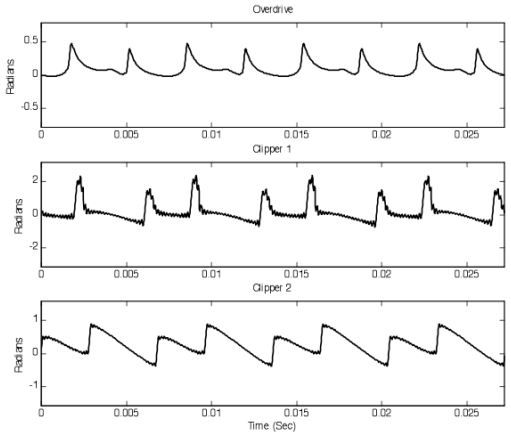

Figure 6: *Phase shaping functions computing using harmonic magnitudes and phases*

Reconstructing the time waveforms from the phase shaping functions given in fig. 6 gives the result in fig. 7. Comparing the waveforms of fig.7 with the originals in fig. 1 they have a good visual match. This demonstrates how amplitude and phase shaping can both produce equivalent results.

4.1. Modelling phaseshapers with Dynamic Time Warping

As an alternative to expressing phaseshaping using eqs. 28-32, it is also possible to represent it as a time warping. This is because of the equivalence of phase and time shifting. This would also obviate the need to find the harmonic magnitudes and phases as the warping can be done explicitly in the time domain. The warping function between the input sine and the distorted wave can be determined using the well-known Dynamic Time Warping algorithm (DTW) [26]. This should be done using single periods of the input sine and the output distorted wave.

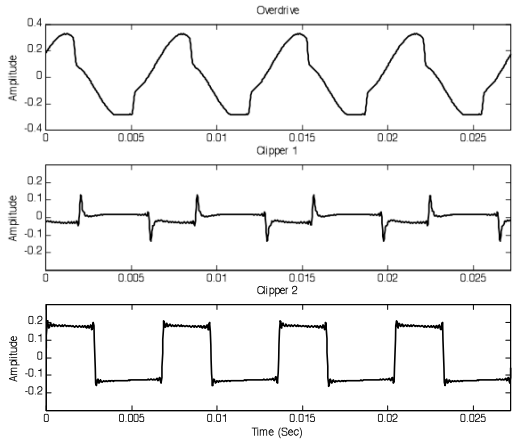

Figure 7 *Reconstructed waveforms using Phase shaping functions derived from harmonic magnitudes and phases*

Denoting the vector of one period of the input sine samples as $\mathbf{x} = \langle x_n \rangle$ and one period of the distorted wave as $\mathbf{y} = \langle y_n \rangle$, with n as the sample index, the goal of applying DTW is to align these two vectors by finding the lowest cost path through the field $\mathbf{F}$, defined as

$$\mathbf{F}_{xy} = d\left(x_n, y_n\right) \tag{39}$$

where $d(.)$ is some appropriate distance metric such as

$$d\left(x_n, y_n\right) = \left|x_n - y_n\right| \tag{40}$$

A matrix $\mathbf{G}$ is defined that contains the accumulated cost in the matching process. A number of different formulas are available for computing $\mathbf{G}$, it was found empirically that the Asymmetric 2 DTW algorithm from [26] performed best. This is defined as

$$\mathbf{G}_{i,j} = \min\begin{cases} \mathbf{G}_{i-1,j-3} + d\left(x_i, y_{j-2}\right) + d\left(x_i, y_{j-1}\right) + d\left(x_i, y_j\right)\big/3 \\ \mathbf{G}_{i-1,j-2} + \left(d\left(x_i, y_{j-1}\right) + d\left(x_i, y_j\right)\right)\big/2 \\ \mathbf{G}_{i-1,j-1} + d\left(x_i, y_j\right) \\ \mathbf{G}_{i-2,j-1} + d\left(x_{i-1}, y_j\right) + d\left(x_i, y_j\right) \\ \mathbf{G}_{i-3,j-1} + d\left(x_{i-2}, y_j\right) + d\left(x_{i-1}, y_j\right) + d\left(x_i, y_j\right) \end{cases} \tag{41}$$

where i and j denote sample indices of x and y respectively.

The upper panel of Fig. 8 illustrates the linear phase plus Phase Shaping function (solid line) for the Overdrive with the DTW warping function (dashed line) superimposed. The match is reasonably good but is not perfect. This is attributable to limitations in the DTW matching process used.

The lower panel of fig. 8 shows the match between the phase shaped emulation of the Overdrive output and a time warped sinewave. The worst alignment is around 5 msec at the most clipped part of the waveform but otherwise it is close. Thus, the match between the two waveforms is better than for the phase, suggesting that small differences in the phase match are not so significant. The main conclusion to draw from this is that the DTW approach has potential but needs more investigation to cre-

ate a refined set of constraints that will improve the performance of DTW for this application.

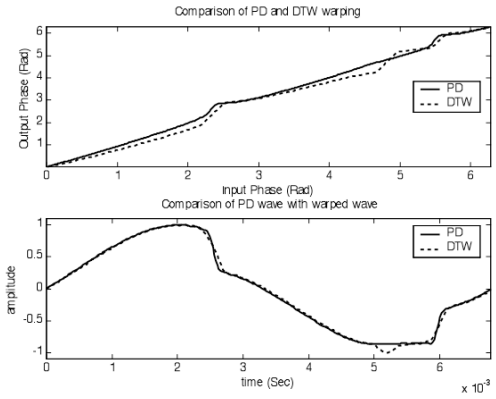

Figure 8: *Phase match between Phase shaped phase for Overdrive (solid line) and DTW algorithm warping function (dashed line) (upper panel) and time waveform match between sine altered by these quantities (lower panel)*

5. DYNAMIC SHAPING ANALYSIS

The shaping functions for both phase and amplitude can be made frequency dependent to create a multiband distortion effect [16]. Although the study so far has been confined to one waveform measurement it should be possible to determine how the waveform shape is affected by the circuitry as the frequency of the input changes. In cases where frequency dependency does not have a significant effect in the output signal, a single shaper could be employed. In other situations, it would be useful to estimate the number of shaping functions required. Such an analysis could be done in the frequency domain but a difficulty is that the number of output signal harmonics diminishes as the frequency increases. An alternative is a time waveform based analysis. A useful tool for this type of measurement is the Scale Transform [27]. In other work, it has been applied to speech spectra analysis for formant normalization [28]. The equation for the scale transform of signal $f(t)$ is

$$D(c) = \frac{1}{\sqrt{2\pi}} \int_0^\infty f(t) e^{\left(-jc-\frac{1}{2}\right)\ln t} dt \qquad (42)$$

The useful property of this transform is that a time scaling of the input will not affect the magnitude of the transform output. A scale modification is a compression or expansion of the time axis of the signal. For example if there is a function $g(t)$ that is a scaled version of $f(t)$ by a factor α

$$g(t) = \sqrt{\alpha} f(\alpha t) \qquad (43)$$

then

$$D_g(c) = \alpha^{jc} D_f(c) \qquad (44)$$

Thus, the transform magnitude is the same for waveforms at different frequencies in that they only differ by a simple scaling factor. To implement the Scale transform the matlab toolbox of [29] was used. This takes the approach of an exponential resampling of the signal followed by an FFT. For the three distortion circuits the output was recorded from frequencies of 82.4 Hz up to 1318.5 Hz, corresponding to a low to high E. All frequencies inbetween were selected to correspond to the notes of the chromatic scale. All measurements were done at the maximum settings of the pedal controls only. One period was extracted from the recorded waveforms and the Scale Transform was found of each. Each Scale Transform was normalised and then all were subtracted from the transform of the first note. The mean square difference for each was found and plotted in fig. 9.

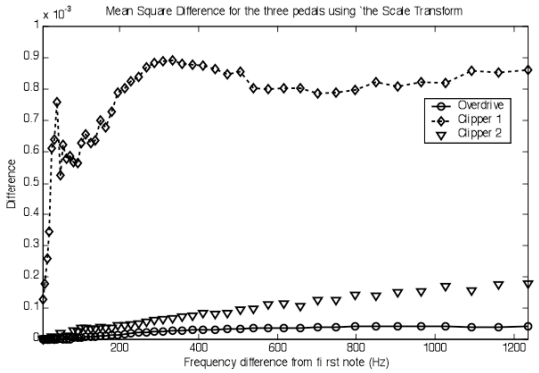

Figure 9: *Scale transform analysis of the distorted waveforms for each circuit with respect to the first measurement*

It appears that the Overdrive is the most consistent in terms of its waveform with respect to frequency. There is a change as the input frequency increases but this flattens out. The change in waveform of Clipper 2 is slightly more pronounced with an increasing difference with respect to input frequency. This could be emulated using a dual-band waveshaper for the low and high frequencies. Clipper 1 has the most significant differences as the input frequency changes, particularly in the low frequency range and would be better represented by a tri-band waveshaper.

To illustrate the changing shape of the output waveforms as indicated by the Scale Transform, Figure 10 plots three periods at the lowest and highest measurement frequencies of 82.41Hz and 1318.5 Hz respectively for Clipper1, upper panels, and Clipper 2, lower panels. The change in waveshape for Clipper 1 from the lowest to highest frequencies is greater than for Clipper 2. This helps in the interpretation of the Scale transform results in Fig. 9.

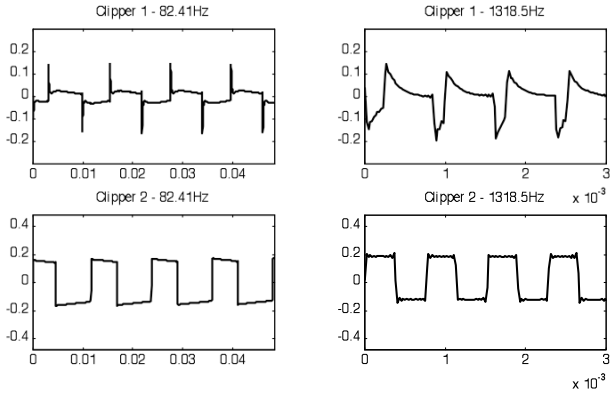

Figure 10: *Waveform outputs from the three distortion circuits fed by a sinewave signal at 1318.5Hz.*

6. CONCLUSION

In this article, we have explored two techniques of signal shaping. Expressions were presented that extended the matrix approach of [19] to include quadrature waveshaping, and to compute a phase shaping function given a set of harmonic magnitudes and phases. These methods were applied to the emulation of distortion effects We were able to demonstrate a good signal match by utilising both amplitude and phase information from spectral analyses in both phase quadrature waveshaping and phase shaping algorithms. In addition, we briefly explored an alternative method of extracting phase distortion functions via Dynamic Time Warping. Finally, the paper described a method of analysing the frequency dependency of shaping functions utilising the Scale transform, which could be of help for the design of multiband distortion effects.

7. ACKNOWLEDGMENTS

This work has been partly funded by the Academy of Finland (project no. 122815).

8. REFERENCES

[1] R.O. Hamm, 'Tubes vs. transistors – is there an audible difference,' *J. Audio Eng. Soc.*, vol. 24, no. 4, pp. 267-273, Sept. 1972.

[2] B. Santo, 'Volume Cranked Up in Amp Debate.' *Electric Engineering Times*, issue 817, Oct. 3, 1998. www.trueaudio.com/at eetjlm.htm [accessed |Apr. 4, 2010].

[3] D. Yeh., J. Abel and J. O. Smith, 'Physically-informed models of distortion and overdrive guitar effect pedals,' *Proceedings of 10th Int. Conference on Digital Audio Effects (DAFx-07)*, Bordeaux, France, September, 2007.

[4] R. Keen, *A musical distortion primer*, http://www.geofex.com/effxfaq/distn101.htm [Accessed: Apr. 4. 2010].

[5] D Yeh. and J. O. Smith, 'Simulating guitar distortion circuits using wave digital and nonlinear state-space formulations,' *Proceedings of 11th Int. Conference on Digital Audio Effects (DAFx-08)*, Espoo, Finland, September, 2008.

[6] J. Schimmel. and J. Misurec, 'Characteristics of broken line approximation and its use in distortion audio effects,' *Proceedings of 10th Int. Conference on Digital Audio Effects (DAFx-07)*, Bordeaux, France, September, 2007.

[7] S. Möller, M. Gromowski and U. Zölzer, 'A measurement technique for highly nonlinear transfer functions,' *Proceedings of 5th Int. Conference on Digital Audio Effects (DAFx-02)*, Hamburg, Germany, September, 2002.

[8] W. Gan and N. Oo, 'Harmonic and intermodulation analysis of nonlinear devices used in virtual bass systems,' *AES Convention 124*, Amsterdam, Netherlands, May 2008.

[9] D. Yeh, *Digital implementation of musical distortion circuits by analysis and simulation*, Ph.D. thesis, Stanford University, Stanford, CA, USA, June 2009. https://ccrma.stanford.edu/~dtyeh/papers/pubs.html [Accessed: Apr. 4. 2010].

[10] T. Hèlie, 'On the use of Volterra series for real-time simulations of weakly nonlinear analog audio devices: application to the Moog ladder filter,' *Proceedings of 9th Int. Conference on Digital Audio Effects (DAFx-06)*, Montreal, Canada, September, 2006.

[11] R.A. Schaefer, 'Electronic musical tone production by nonlinear waveshaping,' *J. Audio Eng. Soc.*, vol. 18, no. 4, pp. 413-417, August 1970.

[12] J. Pekonen, 'Coefficient-modulated first order allpass filter as a distortion effect,' *Proceedings of 11th Int. Conference on Digital Audio Effects (DAFx-08)*, Espoo, Finland, September, 2008.

[13] J. Timoney, V. Lazzarini, J. Pekonen and V. Välimäki, "Spectrally rich phase distortion sound synthesis using an allpass filter", *Proceedings of IEEE ICASSP 2009*, Taipei, Taiwan, 2009, pp. 293-296.

[14] V. Lazzarini and J. Timoney, "New Perspectives on Distortion Synthesis for Virtual Analog Oscillators" *Computer Music Journal 34 (1)*, pp. 28-40, March 2010.

[15] V. Lazzarini, J. Timoney, J. Pekonen and V. Välimäki. "Adaptive Phase Distortion Synthesis," in *Proc. 12th International Conference on Digital Audio Effects* (DAFx'09), Como, Italy, September 1-4, 2009.

[16] P. Fernández-Cid and P. Quirós, 'Distortion of musical signals by means of multiband waveshaping,' *Jnl. of New Music Research*, vol. 30, no. 3, pp. 279-287, Sept, 2001.

[17] J.C. Risset, 'An introductory catalog of computer synthesized sounds', Murray Hill, New Jersey: Bell Laboratories, 1969.

[18] M. LeBrun, "Digital waveshaping synthesis," *J. Audio Eng. Soc.*, vol. 27, no. 4, pp. 250-266, April 1979.

[19] D. Arfib, "Digital synthesis of complex spectra by means of multiplication of nonlinearily distorted sinewaves," *J. Audio Eng. Soc.*, vol. 27, no. 10, pp. 757-768, October 1979.

[20] J. Chowning, "The synthesis of complex audio spectra by means of frequency modulation," *J. Audio Eng. Soc.*, vol. 21, no. 9, pp. 526-534, Sept. 1973.

[21] V. Lazzarini, J. Timoney and T. Lysaght, 'Nonlinear Distortion synthesis using the Split-Sideband method, with applications to adaptive signal processing,' *J. Audio Eng. Soc.*, vol. 56, no. 9, pp. 684-695, Sept. 2008.

[22] W. Nho and P. Laughlin, 'When is instantaneous frequency the average frequency at each time?' *IEEE Sig. Proc. Lett.*, vol. 6, no. 4, pp. 78-80, April. 1999.

[23] L. Rabiner and R. Schafer, *Digital processing of speech signals*, Prentice Hall, Englewood Cliffs, NJ , USA, 1978.

[24] Tonepad: a resource for DIY music projects, http://www.tonepad.com/ [Accessed Apr. 4 2010].

[25] R. Garcia and K. Short, 'Signal analysis using the Complex Spectral Phase Evolution (CSPE) method,' *AES Convention 120*, Paris, France, May 2006.

[26] H. Sakoe and S. Chiba, 'Dynamic programming optimization for spoken word recognition,' *IEEE Trans. on acoustic, ,speech and sig. proc.*, vol. 26, no. 1, pp. 43-49, 1978.

[27] L. Cohen, 'The Scale representation,' *IEEE Trans. On Sig. Proc.*, vol. 41, no. 12, pp. 3275-3292, Dec. 1993.

[28] A. De Sena and D. Rocchesso, 'A study on using the Scale transform for vowel recognition,' *Sound and Music Computing 05*, Salerno, Italy, Nov. 2005.

[29] A. De Sena and D. Rocchesso, 'A fast Mellin and Scale transform," *Eurasip Jnl. on Applied Sig. Proc..*, vol. 2007, no. 1, pp. 1-9, Jan. 2007.